Laser Assisted Catalytic Growth of ZnS/CdSe Core-Shell and Wire-Coil Nanowire Heterostructures

Sheng-Jia Wu (吳盛嘉), Rayapati Venugopal and Yit-Tsong Chen* (陳逸聰)
Department of Chemistry, National Taiwan University, Taipei 106, Taiwan, R.O.C. and
Institute of Atomic and Molecular Sciences, Academia Sinica, P.O. Box 23-166, Taipei 106, Taiwan, R.O.C.

ZnS/CdSe core-shell and wire-coil nanowire heterostructures have been synthesized by chemical vapor deposition assisted with pulsed laser ablation. Measurements from high-resolution transmission electron microscopy and selected area electron diffraction have revealed that both ZnS/CdSe core-shell and wire-coil nanowires are of single-crystalline hexagonal wurtzite structures and grow along the [0001] direction. While the lattice parameters of ZnS and CdSe in the core-shell nanowires are nearly equal to those of bulk ZnS and CdSe, change of the lattice parameters in the CdSe-coil is attributed to the doping of Zn into CdSe, resulting in the relaxation of compressive strain at the interface between CdSe-coil and ZnS-wire. Composition variation across the interfacial regions in the ZnS/CdSe nanowire heterostructures ranges only 10-15 nm despite the pronounced lattice mismatch between ZnS and CdSe by ~11%. Growth mechanisms of the ZnS/CdSe nanowire heterostructures are discussed.

Keywords: Core-shell nanowires; Wire-coil nanowires.

1. INTRODUCTION

One-dimensional (1D) nanoscaled materials are important for fundamental research and technological applications. These materials have a potential to reach higher device densities compared to traditional semiconductor technology. Semiconducting nanowires have been used as building blocks for the assembly of a wide range of nano-devices, including field effect transistors,[1,2] p-n diodes,[2,3] logic gates,[3-5] bipolar transistors, and complementary inverters.[3] 1D heterostructural nanowires with a crystalline and coherent interface along the wire axis hold a great potential for photonic and electronic applications, such as scanning probes, field-emission tips, resonant tunneling devices, nanobarcodes, injection lasers, and thermoelectrics.[3,6-9] However, the success of semiconductor integrated circuits with abrupt interfaces depends largely upon the capability of heterostructural formations through controlled doping and interfacing. It is realized that a pronounced lattice mismatch in the junction area can induce a large strain at the interface and cause degradation in material quality. Despite several recent reports,[10-13] a general synthetic scheme for the formations of 1D nanostructural heterojunctions and superlattices with well defined interfaces is still in its research stage.

In the synthesis of axially modulated nanowire superlattices, a catalyst common to two different materials can be useful to grow a nanowire superlattice structure by modulating the reactants during growth and manipulating the compositional depositions. For instance, Si/SiGe nanowire superlattices with regular modulated compositions were prepared by Wu et al.[10] using a hybrid pulsed laser ablation (PLA)/chemical vapor deposition (CVD) method with Au as a catalyst. Björk et al.[11,12] have fabricated 1D InAs/InP superlattices with atomically sharp interfaces and provided electrical transport data relating to the tunneling of electrons through the heterostructure barriers. Gudiksen et al.[13] synthesized nanowire superlattices of GaAs/GaP with a composition variation across the interface on a length scale comparable to the diameter of the metal-catalyst used in the fabrication.

Epitaxial core-shell and core-multishell nanowire heterostructures of Si and Ge were synthesized by Lauhon et al.[14] using a CVD method. Core-shell heterostructures fabricated from the growth of crystalline overlayers on nanocrystals offer an enhanced emission efficiency[15] and are useful for many applications in biological labels and nanoscaled

Dedicated to Professor Ching-Erh Lin on the Occasion of his 66th Birthday and his Retirement from National Taiwan University

* Corresponding author. E-mail: ytchen@pub.iams.sinica.edu.tw

lasers.[16-18] Quantum dots of CdSe/ZnS core-shell structures have been found to exhibit a lasing effect and can be used for fluoro-immunoassays, biological imaging, and bio-sensors.[19,20] Quantum confinement induced lasing has also been observed in CdSe/ZnS nanorods.[21] However, axial and radial modulations on nanowire structures by compositional doping and morphological variation have so far drawn less attention. In this paper, we discuss the fabrications of ZnS/CdSe core-shell and wire-coil nanowire heterostructures by a PLA/CVD method.

2. EXPERIMENTAL

Apparatus in the PLA/CVD experiments to synthesize ZnS/CdSe nanowire heterostructures is similar to that described in our earlier publications for the fabrications of Si nanowires[22] and CdSe nanobelts and nanosheets.[23] A brief schematic for the PLA/CVD experimental setup is illustrated in Fig. 1a. In the fabrications of ZnS/CdSe nanowire heterostructures, ZnS and CdSe samples (99.999% purity) were separately pressed into pellets by a hydraulic press and were placed in a quartz tube at the upstream of a furnace. Si substrates containing Au nanoparticles were placed downstream of the furnace at different deposition temperatures for the growth of various morphological nanostructures. After evacuating the chamber to < 20 mTorr, the furnace was heated up to 828 °C. The chamber pressure was maintained at ~250 Torr with a constant flow of Ar (90%) and H_2 (10%) at 200 sccm. A pulsed Nd:YAG laser (Spectra Physics GCR-190, 1064 nm wavelength, 7 ns pulse duration, 30 Hz repetition rate, and 15 mJ/pulse) was ignited to ablate the ZnS target. ZnS nanowires were synthesized at ~660 °C.

In the fabrication of ZnS/CdSe core-shell nanowires, the subsequent process was to ablate the CdSe sample to form a CdSe shell on the ZnS wires. The same experimental conditions used for the formation of ZnS nanowires were adopted to ablate the CdSe target except that the deposition of CdSe shell was at different temperatures by placing the growth substrate at an appropriate position inside the furnace as depicted in Fig. 1b. Favorable growth temperature for the CdSe shells was ~380 °C.

For the formation of ZnS/CdSe wire-coil nanowires, procedures of fabricating ZnS nanowires are the same as described above. By comparison, an optimal thermal condition for the CdSe coil growth next to the ZnS wire (whose morphology is shown in Fig. 3b and will be discussed later) was found to be ~470 °C (Fig. 1b).

Morphological, structural, and energy dispersive spectroscopic (EDS) measurements of the as-synthesized ZnS/CdSe nanowire heterostructures have been conducted by scanning electron microscopy (SEM) (LEO 1530 Filed Emission Gun SEM), transmission electron microscopy (TEM), selected area electron diffraction (SAED), and high-resolution TEM (HRTEM) (JEOL JEM 2010 Analytical TEM at 200 kV).

3. RESULTS AND DISCUSSIONS

A. ZnS/CdSe core-shell nanowires

a. Chemical compositions

The as-synthesized ZnS/CdSe core-shell nanowires have diameters of 100-170 nm and can be several μm long observed from SEM images (not shown). Fig. 2a shows a typical TEM morphology where the heterostructural nanowire exhibits a distinct contrast between core and shell. An Au-nanoparticle that attaches on the tip of the nanowire is also

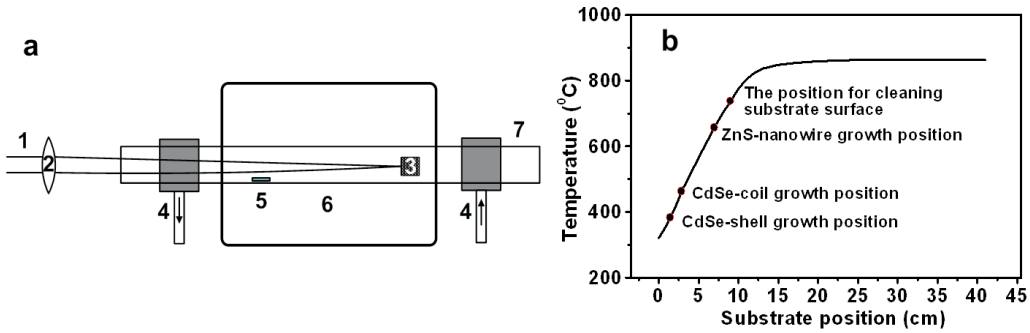

Fig. 1. (a) Schematic illustration of PLA/CVD experimental setup 1. Nd:YAG laser beam, 2. Lens of 100-cm focal length, 3. Target samples, 4. Carrier gases (Ar + H_2) inlet and outlet, 5. Au coated Si substrate, 6. Furnace, 7. Quartz tube. (b) Temperature profile at different substrate positions to the left-side edge of the furnace.

clearly seen. The observed core diameter and shell thicknesses of the heterostructural nanowire are ~47 nm and ~43 nm, respectively.

Elemental analysis for the wire core (Fig. 2b) shows its major compositions of Zn and S with a stoichiometric ratio of 1:1. The weak signals of Cd and Se in Fig. 2b are attributed to the compositions of the wire shell, of which the involvement is inevitable for the electron microscopic investigation of the core structure in the measurement of core-shell nanowires. Chemical analysis on the wire shell (Fig. 2c) indicates that the shell is composed of Cd and Se with a slight contamination of Zn and S. It is noted that the signals of C and Cu originate from a TEM grid. For the particle on the tip of the nanowire, while its shell contains major CdSe and minor ZnS (Fig. 2e), the core of the particle (darker spot in Fig. 2a) is composed of Cd, Se, and Au with minor concentrations of Zn and S (Fig. 2d). The strong signals of Cd and Se in Fig. 2d are likely contributed from the shell for the same reason as described above. Lesser concentrations of Zn and S left in the core of the catalytic Au alloy particle could be due to some reactions involved during the shell formation.

Chemical analysis across the cross-section of the core-shell nanowire with electron beam size of ~2 nm indicates an intermixing compositions of ZnS and CdSe at the core-shell interface. It is interesting to note that the composition variation across the interfacial region between shell and core ranges only 10-15 nm, even though mismatches in the *a* and *c* lattice parameters of ZnS to those of CdSe are 11.14% and 10.74%, respectively. This outcome can be explained by the observation of Gudiksen et al.,[13] in which the composition-variation region with defect-free and atomically abrupt interfaces could be substantially reduced in smaller-diameter

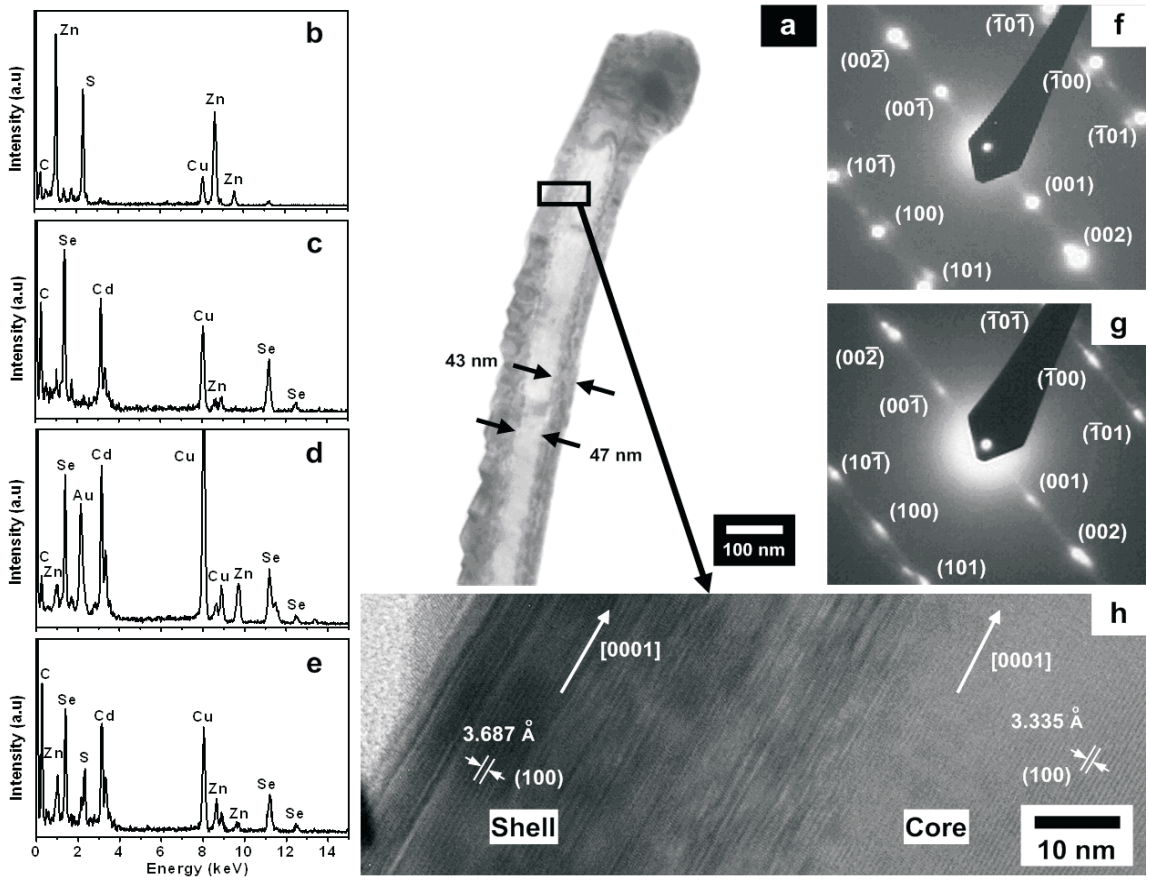

nanowires.

In the reaction to form a CdSe shell on the ZnS nanowires and in order to achieve shorter range of composition variation in the interface, we have tried to pump the ZnS vapor out of the reaction tube prior to the deposition of CdSe shell. Moreover, ZnS vapor was further carried away by the Ar + H_2 mixture carrier after the growth of ZnS nanowires. Meanwhile, the collection substrate of Si wafer was pulled down to a lower temperature region in the furnace. Several minutes later, the substrate was pushed back to an optimal temperature position (Fig. 1b) for the growth of the CdSe shell.

b. Structural determination

The crystalline structures of this core-shell nanowire have been examined by SAED (Figs. 2f-g) and HRTEM (Fig. 2h). These results indicate that both ZnS-core and CdSe-shell have similar single-crystalline hexagonal wurtzite structures. In the SAED patterns, the ED dots show a slight splitting which is caused by a little difference in the lattice parameters between ZnS and CdSe. From our SAED measurements (Figs. 2f-g), the ZnS-core has a single-crystalline hexagonal structure of a = 3.853 Å and c = 6.301 Å. The CdSe-shell is also single-crystalline hexagonal with a = 4.261 Å and c = 6.956 Å. These values agree well with a = 3.820 Å and c = 6.257 Å of bulk ZnS and a = 4.299 Å and c = 7.010 Å of bulk CdSe.

From the HRTEM image (Fig. 2h), we measured $d_{(100)} \approx$ 3.335 Å for the ZnS-core and $d_{(100)} \approx$ 3.687 Å for the CdSe-shell. The obtained interplanar distances of (100) match very well with $d_{(100)\ ZnS}$ = 3.337 Å and $d_{(100)\ CdSe}$ = 3.690 Å calculated from our SAED data. Analysis from the HRTEM (Fig. 2h) indicates that both CdSe-shell and ZnS-core prefer their growths along the [0001] direction. At the interface of ZnS-core and CdSe-shell, we have also observed some roughness by HRTEM. Introducing roughness at the interface is an option for creating single axial dislocation to relieve the strain caused by a lattice mismatch.[24] Some stacking faults were also observed in the CdSe shell of this work.

c. Growth mechanism

In the present work, the formation of ZnS nanowires basically complies with the tip-growth of a vapor-liquid-solid (VLS) model proposed originally by Wagner et al.,[22,23,25] in which a liquid cluster of metal-catalyst provides energetically favored sites for the absorption/adsorption of gas-phase reactants. Sizes of the catalysts are considered to be responsible for the resultant diameters of nanowires. In our experiment, growth of the ZnS nanowires at ~660 °C follows this VLS mechanism, where diameters of the nanowires are basically governed by the sizes of catalytic Au-particles.

The synthesis of CdSe-shell on the ZnS-nanowire takes place at a lower temperature (~380 °C, Fig. 1b) than the formation of ZnS-nanowire (~660 °C). This thermal situation is similar to the formation of Ge-shell on Si nanowires in the fabrication of Ge/Si core-shell nanowires conducted by Lauhon et al.,[14] who have considered an atomic layer epitaxy (ALE) process responsible for the deposition of the shell-structures. It is noteworthy, however, that the CdSe-shell in this work is of single-crystalline nature, unlike the two stage-formation of Ge/Si core-shell single-crystalline nanowires by Lauhon et al.[14] In their fabrication, an amorphous Ge-shell was originally on the single-crystalline Si nanowires, which was crystallized later by annealing.

In this study, the single-crystalline CdSe-shell could have resulted from an *in situ* annealing process. First, owing to a possible rapid ALE, an amorphous or imperfect crystalline CdSe-shell might initially have formed on the surface of ZnS nanowires. Especially, referring to the sizable lattice mismatch between ZnS and CdSe, interfacial defects and imperfect structures were plausible to coexist in the CdSe-shell by the rapid ALE. Second, this metastable CdSe-shell could have transformed to a single-crystalline structure through an *in situ* annealing process. In view of the thermal conditions (< 350 °C) for the synthesis of single-crystalline CdSe nanocrystals reported in several previous studies,[23,26-28] the deposition temperature (~380 °C) of the CdSe-shell in the present work should be high enough to provide sufficient annealing energy for the crystallization of CdSe-shell.

We note that the abruptness in the ZnS/CdSe core-shell interface in the as-synthesized nanostructures is not ideal due to large lattice mismatch. In the experiment, we found that the compositional grading across the interface is strongly dependent on the fine tuning of growth temperature. Chiou et al.[29] also reported a significant improvement at the interface of a GaInP/GaAs quantum well with aid of H_2 purge and PH_3 pre-flow. It is realized that when the lattice mismatch is pronounced, a rough interface with islands and/or dislocations is likely formed at the initial stage of the shell growth due to an increasing strain. In our experiment, islands were not formed at the interface indicating that the strain between core and shell was rather relieved. This outcome is consistent with the interfacial roughness discussed above for the strain relaxation. In our study of core-shell nanowires, while the diameter and length of a ZnS-core depend on the size of a catalytic Au nanoparticle and laser-ablation time, thickness of a CdSe-

shell is only proportional to the growth time.

B. ZnS/CdSe wire-coil nanowires

a. Chemical compositions

Figs. 3a-b show a representative TEM image of a ZnS/CdSe wire-coil nanowire, where a straight nanowire, a helical coil, and a nanoparticle at the junction of wire and coil are observed. EDS analyses (Figs. 3c-e) reveal that while the wire has a stoichiometric ratio of Zn:S ~ 1:1 (Fig. 3c), the coil is composed of Se, Cd, and Zn at a proportion of 50:35:15% (Fig. 3d). This observation suggests that some Zn mixed with CdSe to form the coil structure during the helical growth. To be precise, a compositional formula for the coil should be approximately Cd_2ZnSe_3, indicating that one thirds of Cd in the coil has been substituted by the same II-B group element of Zn compared to the original CdSe bulk sample. In the following discussion, however, we will still represent the helical structure by CdSe-coil for simplicity. Compositional analysis for the nanoparticle at the junction of wire-coil heterostructure (Fig. 3e) reveals its compositions of Au:Cd:Se ~ 47:45:8%. The presence of Au only in the "bridging" nanoparticle, but not in the wire and coil structures, confirms the catalytic nature of Au during the reaction. A similar catalytic metal alloy is also observed by Duan et al.[30] in the laser-

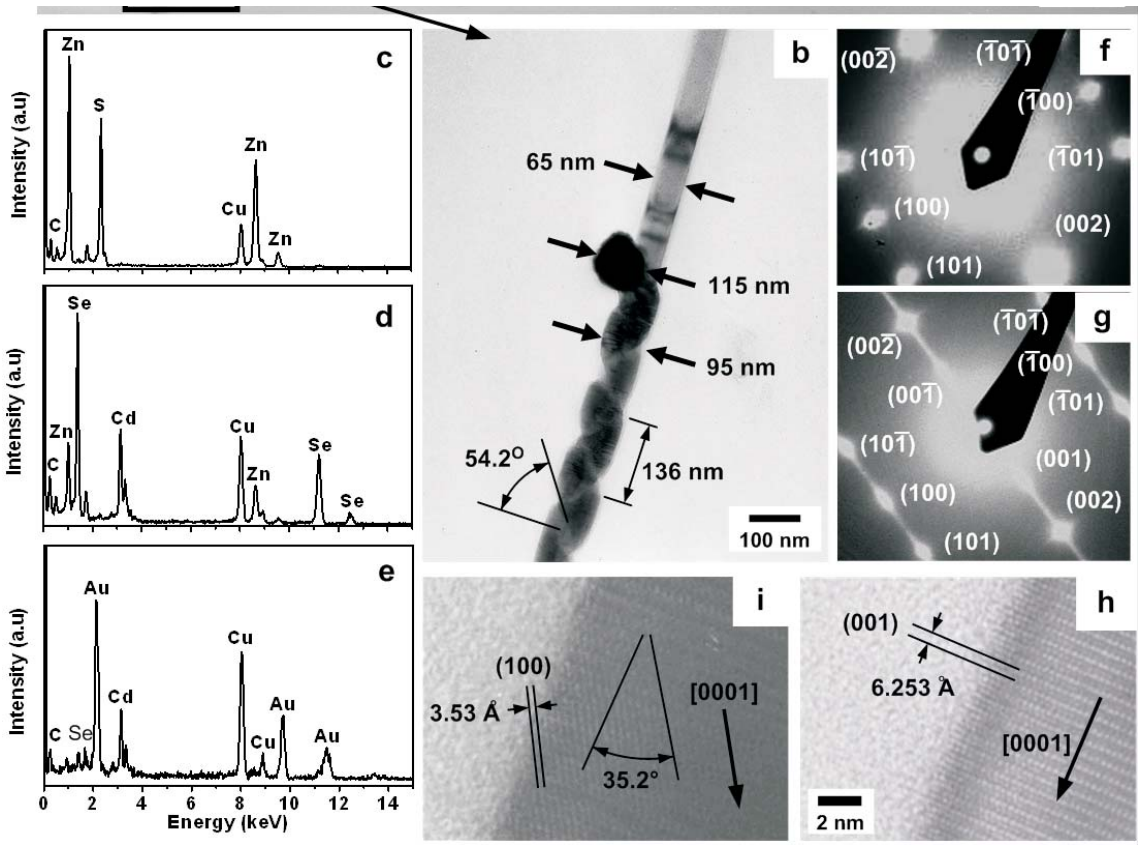

Fig. 3. (a) TEM morphology of a ZnS/CdSe wire-coil nanowire heterostructure. (b) A magnified TEM image of high-contrast ZnS/CdSe wire-coil structure with a straight nanowire (bright contrast, diameter ~65 nm), a helical coil

assisted catalytic growth of single-crystalline GaN nanowires. According to their results, chemical composition of the nanoparticle that attaches to the GaN nanowire is composed of Fe (used as a catalyst), Ga, and N.

b. Structural determination

The SAED results (Fig. 3f-g) show that ZnS/CdSe wire-coil nanowires are of hexagonal wurtzite structure. Calculation for the lattice parameters of the hexagonal ZnS-wire (Fig. 3f) gives a = 3.792 Å and c = 6.255 Å. These values agree well with the standard values of bulk ZnS. On the other hand, the obtained a = 4.080 Å and c = 6.687 Å for the hexagonal CdSe-coil (Fig. 3g) deviate significantly from those of bulk CdSe. The deviation originates from the doping of Zn into CdSe-coil as mentioned earlier. The "bridging" Au-nanoparticle sticks out of the wire-coil nanowire (Fig. 3b), resulting in a substantial contact between ZnS-wire and CdSe-coil at the interface. Because of the significantly different lattice parameters in ZnS and CdSe, the doping of Zn into CdSe-coil has made this lattice mismatch smaller, and has relaxed the strain in the interface to make the heterostructural junction more stable. Composition variation across the interfacial region between wire and coil ranges 12-16 nm. HRTEM images depicted in Figs. 3h-i show clearly single-crystalline structures for the ZnS/CdSe wire-coil nanowire. Both ZnS-wire and CdSe-coil have been observed to grow along the [0001] direction. Interplanar spacings obtained from the HRTEM images of ZnS-wire and CdSe-coil are $d_{(001)\ ZnS} \approx$ 6.253 Å and $d_{(100)\ CdSe} \approx$ 3.530 Å, respectively, consistent with 6.255 Å and 3.533 Å calculated from the SAED results (Figs. 3f-g).

c. Growth mechanisms

The growth of ZnS nanowires is the same as that described earlier and complies with a VLS mechanism. In the subsequent growth of CdSe coil (Fig. 3b), Zn has mixed with CdSe to form the coil structure. Position of the catalytic Au-nanoparticle as shown in Fig. 3b is noteworthy. Displacing from the wire-coil axis and sticking out of the nanowire, the catalytic Au-nanoparticle can therefore have more surface-space to expose to the reactant vapor in the coil growth to carry out a VLS process for the formation of helical structures. In several previous studies for the fabrications of axial heterostructure nanowires,[10-13] a catalytic nanoparticle was always found to locate at the top of a nanowire with each consecutive heterostructure junction either nucleating via an ordinary VLS mechanism,[10-12] or attaching to the open end of the synthesized nanowire.[13] Growth of the ZnS/CdSe wire-coil nanowires in this work, however, is quite unique and different from the previously existing examples. In our study, while the formation of ZnS nanowires complies with a VLS tip-growth mechanism that we have discussed earlier, the growth of CdSe-coils follows a root-growth mechanism as evidenced by the distinct position of catalytic Au-nanoparticle at the junction of heterostructural nanowires (Fig. 3b). The root-growth in this work probably stems from the lattice mismatch between ZnS and CdSe by ~11%, which is quite pronounced compared to 3.42% in a previous case of GaP/GaAs nanowire superlattices fabricated by Gudiksen et al.[13] Because of the sizable lattice mismatch between ZnS and CdSe, the deposition of CdSe is more favorable to the catalytic Au-nanoparticle than to the open end of the already formed ZnS-wire. It is also interesting to note that unlike the previous nanowire-superlattice examples where the nucleation of heterostructure junctions is in the same direction to the Au-nanoparticle,[10-13] a helical structure formed in this experiment was in the opposite direction with the Au-nanoparticle lying in the middle as a joint (Fig. 3b).

In the same line of reasoning to ease the compressive strain in the interface of ZnS-wire and CdSe-coil, leak of Zn into the CdSe-coil to make the mismatch of lattice parameters smaller was an option to relax the strain. The supply of Zn could come from the residual ZnS vapor in the reaction tube, or at the expense of melting the already formed ZnS nanowires. Moreover, doping of Zn into the growing CdSe-coil could have been mediated by the Au catalyst. In view of the dissolutions between the reactants (Cd, Se, Zn, and S) and catalyst (Au), an order of mixing with Au at ~470 °C is Cd > Zn > Se > S based on their phase-diagram data.[31] However, the laser-ablated Cd and Se vapors are prevailing during the coil growth, resulting in an approximate composition of Cd_2ZnSe_3 for the coil structure determined by EDS (Fig. 3d). A lacking of S in the coil could be due to the high volatility of S and/or its low solubility with Au during the coil growth. Accordingly, S could escape from the surface of an Au-nanoparticle and, as a consequence, S is absent in the coil (Fig. 3d).

The CdSe-coil is an intriguing structure fabricated in the present study. To date, there are several growth mechanisms proposed for the formations of helical nanowires and nanotubes.[32-34] To explain the formation of boron-carbide nanosprings, McIlroy et al.[33] have put forward a contact angle anisotropy (CAA) model, where helical growth is due to anisotropic growth rates around the perimeter of catalyst/wire interface resulting from various surface-energy at different catalyst/wire contact angle.

In this work, the catalytic Au-nanoparticle has been observed to protrude from the junction in the ZnS/CdSe wire-

coil heterostructures. Sticking out of the wire-coil axis rather than being embedded in the nanowire, the Au-nanoparticle thus has more surface-space to expose to the reactant vapor to catalyze the helical growth via a VLS mechanism. In the growth of CdSe-coil, asymmetric extruding of the helical wire (diameter ~88 nm) from the catalytic Au-alloy liquid-droplet (diameter ~115 nm, Fig. 3b) can be nicely accounted for by the CAA model,[33] where an apparent displacement between CdSe wire-axis and Au particle-center has driven the spiral growth via a VLS process. In our study, right- or left-handed chirality in the fabricated CdSe-coils is distributed equally statistically, rendering a racemic mixture. It is also remarkable that the pitch angle of ~54.2° in the CdSe-coil (Fig. 3b) coincides with one of the two distinct pitch angles, ~54° and ~11°, observed in helical ribbons as intermediates in the crystallization of cholesterol.[35] These helical structures with high- and low-pitch angles of ~54° and ~11°, respectively, have also been shown to be general features[36-39] in not only the model bile systems,[35] but also a variety of four-component systems composed of a bile salt or nonionic detergent, a phosphatidylcholine or fatty acids, a steroid analog of cholesterol, and water.[40]

4. CONCLUSION

ZnS/CdSe core-shell and wire-coil nanowire heterostructures have been fabricated by a PLA/CVD method. HRTEM and SAED results have indicated that the as-synthesized core-shell and wire-coil nanowires are of single-crystalline hexagonal wurtzite structures. For the core-shell structure, the lattice parameters of ZnS/CdSe nanowires are nearly equal to those of bulk ZnS and CdSe. HRTEM images reveal that both ZnS-core and CdSe-shell prefer growing along the [0001] direction. For the wire-coil structure, variation of the lattice parameters in the CdSe-coil is attributed to the doping of Zn into CdSe, resulting in the relaxation of the compressive interfacial strain between CdSe-coil and ZnS-wire. The growth directions for the ZnS-wire and CdSe-coil are both parallel to the [0001] direction. Proposed growth mechanisms of the ZnS/CdSe core-shell and wire-coil nanowire heterostructures have been discussed.

ACKNOWLEDGMENTS

This work is supported by the National Science Council of ROC (Grant Nos. 93-2113-M-002-027 and 93-2120-M-002-001) and CTCI Foundation. This paper has been prepared for the special issue in the Journal of the Chinese Chemical Society dedicated to honor Professor Chin-Erh Lin's retirement from National Taiwan University.

Received February 4, 2005.

REFERENCES

1. Cui, Y.; Duan, X.; Hu, J.; Lieber, C. M. *J. Phys. Chem. B* **2000**, *104*, 5213.
2. Duan, X.; Huang, Y.; Cui, Y.; Wang, J.; Lieber, C. M. *Nature* **2001**, *409*, 66.
3. Cui, Y.; Lieber, C. M. *Science* **2001**, *291*, 851.
4. Huang, Y.; Duan, X.; Cui, Y.; Lauhon, L. J.; Kim, K.-H.; Lieber, C. M. *Science* **2001**, *294*, 1313.
5. Bachtold, A.; Hadley, P.; Nakanishi, T.; Dekker, C. *Science* **2001**, *294*, 1317.
6. Hu, J.; Odom, T. W.; Lieber, C. M. *Acc. Chem. Res*. **1999**, *32*, 435.
7. Holmes, J. D.; Johnston, K. P.; Doty, R. C.; Korgel, B. A. *Science* **2000**, *287*, 1471.
8. Favier, F.; Walter, E. C.; Zach, M. P.; Benter, T.; Penenr, R. M. *Science* **2001**, *293*, 2227.
9. Huang, M.; Mao, S.; Feick, H.; Yan, H.; Wu, Y.; Kind, H.; Weber, E.; Russo, R.; Yang, P. *Science* **2001**, *292*, 1897.
10. Wu, Y. Y.; Fan, R.; Yang, P. D. *Nano Lett*. **2002**, *2*, 83.
11. Björk, M. T.; Ohlsson, B. J.; Sass, T.; Persson, A. I.; Thelander, C.; Magnusson, M. H.; Deppert, K.; Wallenberg, L. R.; Samuelson, L. *Nano Lett*. **2002**, *2*, 87.
12. Björk, M. T.; Ohlsson, B. J.; Sass, T.; Persson, A. I.; Thelander, C.; Magnusson, M. H.; Deppert, K.; Wallenberg, L. R.; Samuelson, L. *Appl. Phys. Lett*. **2002**, *80*, 1058.
13. Gudiksen, M. S.; Lauhon, L. J.; Wang, J.; Smith, D. C.; Lieber, C. M. *Nature* **2002**, *415*, 617.
14. Lauhon, L. J.; Gudiksen, M. S.; Wang, Deli; Lieber, C. M. *Nature* **2002**, *420*, 57.
15. Nirmal, M.; Brus, L. *Acc. Chem. Res*. **1999**, *32*, 407.
16. Bruchez, M.; Moronne, M.; Gin, P.; Weiss, S.; Alivisatos, A. P. *Science*, **1998**, *281*, 2013.
17. Chan, W. C.; Nie, S. M. *Science* **1998**, *281*, 2016.
18. Klimov, V. I.; Mikhailovsky, A. A.; Xu, S.; Malko, A.; Hollingsworth, J. A.; Leatherdale, C. A.; Eisler, H.-J.; Bawendi, M. G. *Science* **2000**, *290*, 314.
19. Tran, P. T.; Goldman, E. R.; Anderson, G. P.; Mauro, J. M.; Mattoussi, H. *Phys. Status Solidi. B* **2002**, *229*, 427.
20. Goldman, E. R.; Balighian, E. D.; Mattoussi, H.; Kuno, M. K.; Mauro, J. M.; Tran, P. T.; Anderson, G. P. *J. Am. Chem. Soc*. **2002**, *124*, 6378.
21. Kazes, M.; Lewis, D. Y.; Ebenstein, Y.; Mokari, T.; Banin, U.

Adv. Mater. **2002**, *14*, 317.
22. Yang, Y.-H.; Wu, S.-J.; Chiu, H.-S.; Lin, P.-I.; Chen, Y.-T. *J. Phys. Chem. B* **2004**, *108*, 846.
23. Venugopal, R.; Lin, P.-I.; Liu, C.-C.; Chen, Y.-T. *J. Am. Chem. Soc.* **2005**.
24. Wang, Y. Q.; Wang, Z. L.; Brown, T.; Brown, A.; May, G. *Thin Solid Films* **2001**, *397*, 162.
25. Wagner, R. S.; Ellis, W. C. *Appl. Phys. Lett*. **1964**, *4*, 89.
26. Maehashi, K.; Yasui, N.; Ota, T.; Noma, T.; Murase, Y.; Nakashima, H. *J. Cryst. Growth* **2001**, *227-228*, 1116.
27. Matsumura, N.; Saito, T.; Saraie, J. *J. Cryst. Growth* **2001**, *227-228*, 1121.
28. Qu, L.; Peng, X. *J. Am. Chem. Soc*. **2002**, *124*, 2049.
29. Chiou, S. W.; Lee, C. P.; Hong, J. M.; Chen, C. W.; Tsou, Y. *J. Cryst. Growth*. **1999**, *206*, 166.
30. Duan, X.; Lieber, C. M. *J. Am. Chem. Soc*. **2000**, *122*, 188.
31. Phase diagrams can be found in Pauling File (http://crystdb.nims.go.jp/).
32. Amelinckx, S.; Zhang, X. B.; Bernaerts, D.; Zhang, X. F.; Ivanov, V.; Nagy, J. B. *Science* **1994**, *265*, 635.
33. Mcllroy, D. N.; Zhang, D.; Kranov, Y.; Norton, M. G. *Appl. Phys. Lett*. **2001**, *79*, 1540.
34. Motojima, S.; Chen, Q. *J. Appl. Phys*. **1999**, *85*, 3919.
35. Chung, D. S.; Benedek, G. B.; Konikoff, F. M.; Donovan, J. M. *Proc. Natl. Acad. Sci. USA* **1993**, *90*, 11341.
36. Helfrich, W. *J. Chem. Phys.* **1986**, *85*, 1085.
37. Helfrich, W.; Prost, J. *Phys. Rev. A* **1988**, *38*, 3065.
38. Schnur, J. M. *Science*, **1993**, *262*, 1669.
39. Komura, S.; Ou-Yang, Z.-C. *Phys. Rev. Lett.* **1998**, *81*, 473.
40. Smith, B.; Zastavker, Y. V.; Benedek, G. B. *Phys. Rev. Lett*. **2001**, *87*, 278101.